

## Computational Studies of Nucleophilic Substitution at Carbonyl Carbon: the S<sub>N</sub>2 Mechanism versus the Tetrahedral Intermediate in Organic Synthesis

Joseph M. Fox, Olga Dmitrenko, Lian-an Liao, and Robert D. Bach\*

Brown Laboratories, Department of Chemistry and Biochemistry, University of Delaware,  
Newark, Delaware 19803

rbach@udel.edu

Received March 28, 2004

A theoretical study specifically addresses the question of whether nucleophilic addition to the carbonyl groups of acid chlorides, esters, and anhydrides involves an addition–elimination pathway or proceeds by a concerted S<sub>N</sub>2-like mechanism in the absence of the generally assumed tetrahedral intermediate. Density functional calculations [B3LYP/6-31+G(d,p)] establish that chloride ion exchange reactions with both formyl and acetyl chloride proceed by a  $\pi$  attack on the C=O bond. No discernible tetrahedral intermediate typical of an addition–elimination pathway was found in either case. While a tetrahedral intermediate does exist for the addition of fluoride ion to (Cl)<sub>2</sub>C=O, halide exchange of LiCl with both ClFC=O and (Cl)<sub>2</sub>C=O also proceeds by a concerted S<sub>N</sub>2-like pathway. The formation of a tetrahedral intermediate from the addition of methanol to acetyl chloride is slightly exothermic (4.4 kcal/mol). The ion–dipole complex of methanol weakly bonded to the carbonyl carbon of protonated acetyl chloride is stabilized by 13.8 kcal/mol but does not collapse to a tetrahedral intermediate. When four CH<sub>3</sub>OH molecules are H-bonded to protonated acetyl chloride, a tetrahedral intermediate is not completely formed and this solvated complex more closely resembles the precursor to an S<sub>N</sub>1-type ionization of Cl<sup>−</sup>. With six H-bonding methanol molecules, a methanol adds to the carbonyl carbon and a proton relay occurs with formation of a tetrahedral-like structure that immediately loses chloride ion in an S<sub>N</sub>1-like solvolysis. These results corroborate earlier suggestions (Bentley et al. *J. Org. Chem.* **1996**, *61*, 7927) that the methanolysis of acetyl chloride does not proceed through the generally assumed addition–elimination pathway with a discrete tetrahedral intermediate but is consistent with ionization of Cl<sup>−</sup>. The reaction of methoxide ion with methyl acetate proceeds via a multiple-well energy surface and involves the intermediacy of an asymmetrical species with differing C–OMe bond lengths. Models of synthetic applications of acyl transfer reactions involving anhydrides that form *N*-acyloxazolidinones also proceed by a concerted S<sub>N</sub>2-type pathway even with the carboxylate leaving group. Concerted transition states were observed for the reactions of each enantiomer of a 1,3-diphenylcycloprop-2-ene carboxylic anhydride by *S*-3-lithio-4-phenyloxazolidinone. Despite close structural similarities between the diastereomeric transition states, the relative energies correlated closely with the experimental results.

### I. Introduction

The intermediacy of a tetrahedral species is usually considered to be the rule for acyl transfer processes, and the textbook perception<sup>1</sup> is that concerted S<sub>N</sub>2-type mechanisms<sup>2</sup> occur only in exceptional cases. The <sup>18</sup>O labeling experiments by Bender<sup>3</sup> provided evidence for a tetrahedral intermediate in hydrolysis of a number of carboxylic esters, and since then it has been evidenced that acyl transfer reactions with strong nucleophiles and poor leaving groups typically proceed via an associa-

tive complex.<sup>4,5</sup> However, the generality of the tetrahedral intermediate has been in question since Bender et al.<sup>6</sup> reported that benzyl benzoates, unlike alkyl benzoates, do not incorporate <sup>18</sup>O during alkaline hydrolysis. Shain and Kirsch<sup>7</sup> later questioned some of the experiments by Bender regarding <sup>18</sup>O exchange with alkyl benzoates. McClelland<sup>8</sup> measured the rate constant for the breakdown of an anionic hemi-ortho ester to be  $\sim 5 \times 10^7$ , which is faster than proton transfer, and he pointed out that, for leaving groups better than alkoxide, the lifetime of the tetrahedral intermediate would be too short to exist.

(1) (a) March, J. *Advanced Organic Chemistry*, 4th ed.; Wiley: New York, 1992; pp 330–335. (b) Lowry, T. H.; Richardson, K. S. *Mechanism and Theory in Organic Chemistry*, 3rd ed.; Harper and Row: New York, 1987.

(2) For an excellent treatment of the literature of acyl transfer mechanisms and for experimental support of S<sub>N</sub>2 mechanisms in solvolysis reactions of acyl chlorides, see Bentley, T. W.; Llewellyn, G.; McAlister, J. A. *J. Org. Chem.* **1996**, *61*, 7927.

(3) Bender, M. L. *J. Am. Chem. Soc.* **1951**, *73*, 1626.

(4) Capon, B.; Ghosh, A. K.; Grieve, D. M. A. *Acc. Chem. Res.* **1981**, *14*, 306.

(5) McClelland, R. A.; Santry, L. J. *Acc. Chem. Res.* **1983**, *16*, 394.

(6) Bender, M. L.; Matsui, H.; Thomas, R. J.; Tobey, S. W. *J. Am. Chem. Soc.* **1961**, *83*, 4193.

(7) Shain, S. A.; Kirsch, J. F. *J. Am. Chem. Soc.* **1968**, *90*, 5848.

(8) McClelland, R. A. *J. Am. Chem. Soc.* **1984**, *106*, 7579.

Experimental support for concerted mechanisms of acyl transfer has been evidenced by a number of groups. Elegant studies by Williams and co-workers<sup>9–11</sup> have shown that the Brønsted dependence for attack of phenoxides on 4-nitrophenylacetate is linear and therefore inconsistent with a mechanism that involves a tetrahedral intermediate. Chrystiuk and Williams<sup>12a</sup> reached a similar conclusion for the displacement of isoquinoline from *N*-(methoxycarbonyl)isoquinolinium ion by pyridine nucleophiles, and in more recent experimental work Um, Buncel, and co-workers<sup>12b</sup> have rejected the tetrahedral intermediate for the reactions of anionic nucleophiles with aryl benzoates. Brauman and co-workers<sup>13–16</sup> later argued that for gas-phase reactions the tetrahedral structure is not located at the energy minimum but at the saddle point for many nucleophilic displacements. They interpreted their ion cyclotron resonance data as supporting double-well energy surfaces with ion–dipole complexes as the intermediates. On the basis of pulsed ICR techniques, Kim and Caserio<sup>17</sup> also questioned the generality of this mechanism in gas phase, where a series of acyl transfer reactions were demonstrated to proceed through acylium ion complexes rather than the more commonly anticipated addition–elimination pathway. Guthrie<sup>18</sup> has also proposed a concerted mechanism for the alcoholysis of certain esters, and there is evidence that the solvolysis of some acyl chlorides occurs by a concerted process.<sup>2,19,20</sup>

Earlier theoretical gas-phase studies by Yamabe and Minato<sup>21</sup> showed that rather simple acyl transfer reactions between chloride ion and acetyl chloride take place in a concerted fashion in the absence of a tetrahedral intermediate. Blake and Jorgensen<sup>22</sup> also reported ab initio calculations on the degenerate exchange reactions of Cl<sup>−</sup> with HCOCl and CH<sub>3</sub>COCl and found tetrahedral transition states for both nucleophilic displacement reactions. More recently, Lee and co-workers<sup>23</sup> have reported on acyl transfer mechanisms for a variety of carbonyl compounds including thiocarbonyl, sulfonyl, and phosphoryl derivatives. They found that the backside  $\sigma$  attack pathway was only favored over a  $\pi$  route when the carbon-bound leaving group had a low-lying  $\sigma^*$  orbital.

To date, the computational work on concerted acyl transfer mechanisms has focused only on calculations in the gas phase. For utility in synthetic chemistry, sys-

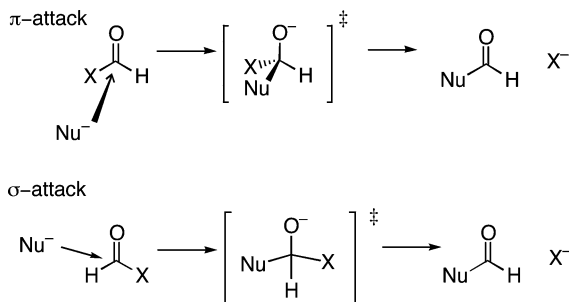
tematic studies that use high-level calculations should also consider the effects of solvation and catalysis. Furthermore, it must also be demonstrated that high-level calculations can be applied to complex reactants. We have reexamined the fundamental question of acyl transfer using density functional theory (DFT) and now extend these studies to acyl transfer reactions that form *N*-acyloxazolidinones with specific applications in complex molecule synthesis.<sup>24,25</sup> The reactions of acid halides, anhydrides, and esters were studied by use of gas-phase calculations and solvent-containing models. The work here considers halogen, alkoxide, and nitrogenous nucleophiles. Acyl transfer reactions of anhydrides with oxazolidinones are known to be catalyzed by the addition of LiCl, and our calculations explicitly examine the role of catalysis on the reaction mechanism. In most cases, the conclusion reached is that the reactions are concerted S<sub>N</sub>2-type processes that do not proceed through tetrahedral intermediates. These findings contradict the conventional wisdom that continues to invoke the tetrahedral intermediate mechanism in almost every situation and S<sub>N</sub>2 or concerted mechanisms only for unique or unusual substrates. The body of evidence presented here shows that the tetrahedral intermediate mechanism is hardly a rule, and for different combinations of nucleophiles and electrophiles it is by no means straightforward to predict the mechanism of this seemingly simple process. This fundamental mechanistic question concerning acyl transfer is particularly relevant today since many enzyme-catalyzed acyl transfer reactions take place within the hydrophobic reaction environment at the active site of the enzyme. Furthermore, many synthetically useful enantioselective kinetic resolution and desymmetrization processes involve acyl transfer,<sup>26–29</sup> and it is obviously impossible to rationalize and improve the selectivity of such processes if the incorrect mechanism is invoked. Accordingly, there is a need for high-level theoretical studies on acyl transfer reactions of simple systems under varied conditions (with both gas-phase and solvent models) and to demonstrate that these methods can be applied to complex systems of synthetic interest. The fundamental studies that follow are a prerequisite to a better understanding of the more complex explanation of diastereoselectivity of the acyl transfer processes involved in organic syntheses.

## II. Results and Discussion

**II.1. Single-Step S<sub>N</sub>2  $\pi$  Attack versus an Addition–Elimination Pathway.** In an acyl transfer reaction, the *concerted* displacement of a nucleofuge can occur by one of the two basic approaches depicted in Scheme 1. The  $\pi$  approach involves out-of-plane nucleophilic attack on the  $\pi^*$  orbital of the carbonyl group to give a tetrahedral *transition state*. A second avenue for concerted acyl transfer involves in-plane nucleophilic attack

- (9) Williams, A. *Acc. Chem. Res.* **1989**, *22*, 387.  
(10) Ba-Saif, S.; Luthra, A. K.; Williams, A. *J. Am. Chem. Soc.* **1989**, *111*, 2647.  
(11) Ba-Saif, S.; Luthra, A. K.; Williams, A. *J. Am. Chem. Soc.* **1987**, *109*, 6362.  
(12) (a) Chrystiuk, E.; Williams, A. *J. Am. Chem. Soc.* **1987**, *109*, 3040. (b) Um, I. H.; Han, H. J.; Ahn, J. A.; Kang, S.; Buncel, E. *J. Org. Chem.* **2002**, *67*, 8475.  
(13) Wilbur, J. L.; Brauman, J. I. *J. Am. Chem. Soc.* **1994**, *116*, 9216.  
(14) Wilbur, J. L.; Brauman, J. I. *J. Am. Chem. Soc.* **1994**, *116*, 5839.  
(15) Craig, S. L.; Zhong, M.; Brauman, J. I. *J. Am. Chem. Soc.* **1999**, *121*, 11790.  
(16) Zhong, M.; Brauman, J. I. *J. Am. Chem. Soc.* **1999**, *121*, 2508.  
(17) Kim, J. K.; Caserio, M. C. *J. Am. Chem. Soc.* **1981**, *103*, 2124.  
(18) Guthrie, J. P. *J. Am. Chem. Soc.* **1991**, *113*, 3941.  
(19) Kevill, D. N.; Kim, C. B. *J. Chem. Soc., Perkin Trans. 2* **1988**, *7*, 1353.  
(20) Bentley, T. W.; Harris, H. C. *J. Chem. Soc., Perkin Trans. 2* **1986**, 619.  
(21) Yamabe, S.; Minato, T. *J. Org. Chem.* **1983**, *48*, 2972.  
(22) Blake, J. F.; Jorgenson, W. L. *J. Am. Chem. Soc.* **1987**, *109*, 3856.  
(23) Lee, I.; Kim, C. K.; Li, H. G.; Sohn, C. K.; Kim, C. K.; Lee, H. W.; Lee, B.-S. *J. Am. Chem. Soc.* **2000**, *122*, 11162.

- (24) Liao, L.-a.; Fox, J. M. *J. Am. Chem. Soc.* **2002**, *124*, 14322.  
(25) Liao, L.-a.; Zhang, F.; Yan, N.; Golen, J. A.; Fox, J. M. *Tetrahedron* **2004**, *60*, 1803.  
(26) Vedejs, E.; Daugulis, O.; Mackay, J. A.; Rozners, E. *Synlett* **2001**, 1499.  
(27) Spivey, A. C.; Maddaford, A.; Redgrave, A. *J. Org. Prep. Proced. Int.* **2000**, *32*, 331.  
(28) Fu, G. C. *Acc. Chem. Res.* **2000**, *33*, 412.  
(29) Willis, M. C. *J. Chem. Soc., Perkin Trans. 1* **1999**, 1765.

**SCHEME 1. Concerted Mechanisms for Acyl Transfer**

on the C–X  $\sigma^*$  orbital. The out-of-plane mechanism draws close analogy to the commonly accepted addition–elimination mechanism for acyl transfer, except for the involvement of a transition state instead of a tetrahedral intermediate. However, recent studies on the nucleophilic substitution reactions of vinyl halides mandate that serious consideration must be given to the  $\sigma$  approach as well. Studies at the G2(+) level of theory<sup>30a</sup> suggested that unactivated vinyl substrates such as vinyl chloride could afford gas-phase, single-step halide exchange by a pure in-plane  $\sigma$  approach of the nucleophile to the backside of the C–Cl  $\sigma$  bond. A subsequent high-level computational study using CCSD, CCSD(T), and G2(+) methods<sup>30b</sup> established that the in-plane gas-phase  $\sigma$  approach of chloride ion to vinyl chloride is favored over the more classical  $\pi$  approach by 5.9 kcal/mol at the G2(+) level of theory. However, this appears to be an isolated example since the  $\pi$  approach is favored for more activated alkenyl halides.<sup>30b</sup> It is clear that any study of acyl transfer reactions must analyze both types of concerted displacements in addition to the stepwise pathway.

**(a) Degenerate Chloride Ion Exchange.** At the B3LYP/6-31+G(d,p) level of theory the degenerate exchange of Cl<sup>−</sup> with HCOCl does proceed by a concerted pathway involving  $\pi$  attack with a relatively low activation barrier [ $\Delta(E + \text{ZPVE})^\ddagger = 9.2$  kcal/mol]. The out-of-plane ( $S_N\pi$ ) pathway is a first-order saddle point that has  $C_s$  symmetry. The incoming nucleophile and leaving group are each bonded to distinct,  $\sim sp^3$  carbon orbitals of the approximate tetrahedral *transition state* (see

Supporting Information, Figure S1). A similar transition structure was observed with Cl<sup>−</sup> exchange with CH<sub>3</sub>COCl (Figure 1). The classical activation barrier for concerted  $\pi$  attack [ $\Delta(E + \text{ZPVE})^\ddagger = 8.8$  kcal/mol] is much preferred to the in-plane second-order halide exchange reaction (Figure 1). *No evidence for the existence of a tetrahedral intermediate was observed in either case.*

In general, a “concerted” reaction involves two (or more) bond making or breaking processes that occur synchronously as the reaction proceeds. This implies that there is no discrete or discernible intermediate with a finite lifetime along the reaction coordinate. The in-plane ( $S_N\sigma$ ) pathway has geometrical implications imposed by the  $\sigma$  symmetry plane since the nucleophile and the leaving group in this planar array are both partially bonded to the carbonyl carbon in an  $S_N2$  sense with opposite lobes of a single p orbital on carbon. For the HCOCl and CH<sub>3</sub>COCl in-plane  $\sigma$  attack of Cl<sup>−</sup>, the two chloride atoms deviate from linearity with a Cl–C–Cl angle of 142.0° and 168.4° (Figures 1 and S1). This approach, however, is a second-order saddle point<sup>31</sup> and in both cases the in-plane  $\sigma$  attack has a much higher activation energy [ $\Delta\Delta(E + \text{ZPVE})^\ddagger = 13.2$  and 14.7 kcal/mol]. Thus, in contrast to Cl<sup>−</sup> exchange with vinyl chloride,<sup>30</sup> displacement with the simplest acid chloride also proceeds by the  $\pi$  route in the absence of a tetrahedral intermediate.

When should one anticipate a stable tetrahedral intermediate? In general, a delicate balance exists between the energy of the  $\pi$ -bond component of the initial carbonyl  $\pi$  bond, the C–X bond strength of the incoming nucleophile, and the stability of the leaving group. In the case of a very strong developing C–F bond, such as F<sup>−</sup> addition to phosgene (Figure 2), an approximate tetrahedral intermediate does exist but the C–Cl bonds are atypically long (2.003 Å).

This anionic intermediate has a stabilization energy of −54.7 kcal/mol relative to its reactants. In contrast when the concerted displacement of Cl<sup>−</sup> by LiF involves a neutral complex, the stabilization energy is much lower ( $\Delta E_{\text{stab}} = -10.2$  kcal/mol). The reaction has an activation barrier of only 3.2 kcal/mol since the fluoride is ideally poised in the ground-state (GS) complex to displace Cl<sup>−</sup> (Figure 3). The degenerate exchange of LiCl with

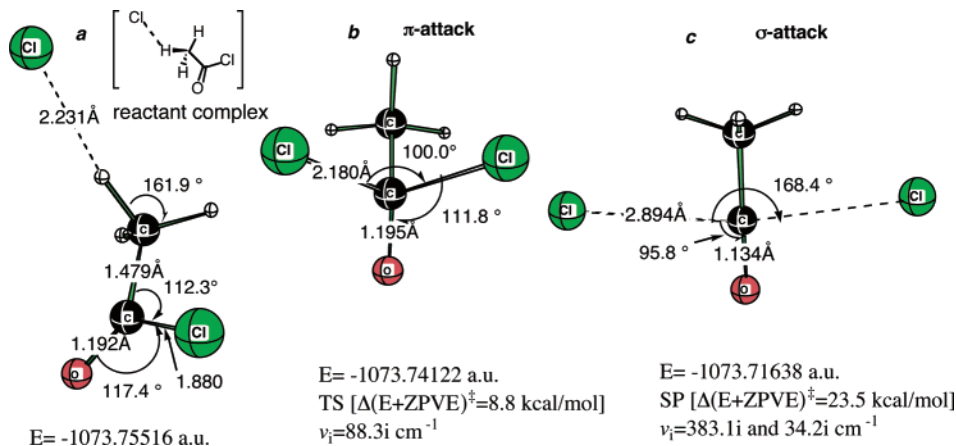


**FIGURE 1.** Exchange reaction of Cl<sup>−</sup> with CH<sub>3</sub>COCl: (a) energy minimum; (b)  $\pi$  attack, a transition structure (TS); (c) an in-plane  $\sigma$  attack, a second-order saddle point (SP). All structures are optimized at the B3LYP/6-31+G(d,p) level. Imaginary frequencies and zero-point vibrational energies (ZPVE) are at the B3LYP/6-31G(d) level.



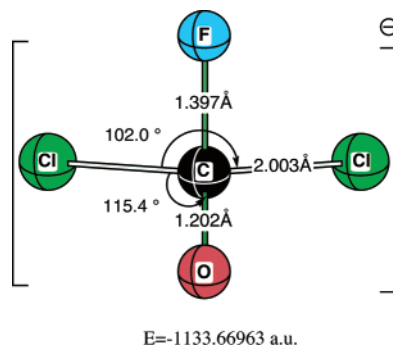


**FIGURE 2.** Tetrahedral intermediate from the addition of  $F^-$  to  $(Cl)_2C=O$  optimized at the B3LYP/6-31+G(d,p) level of theory.

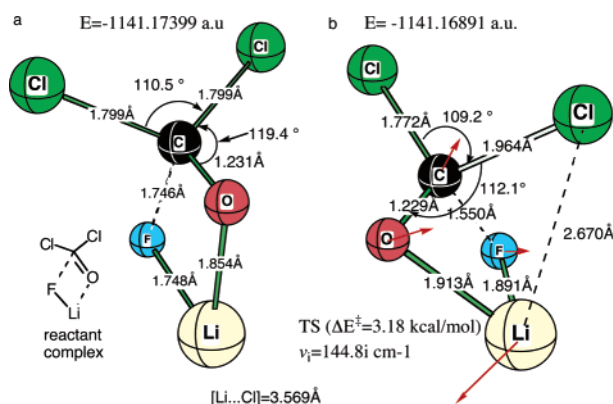


**FIGURE 3.** Exchange reaction of LiF with  $(Cl)_2C=O$ :  $LiF + (Cl)_2C=O \rightarrow LiCl + ClFC=O$ . Reactant complex (a) and transition structure (b) are optimized at the B3LYP/6-31+G(d,p) level. Imaginary frequency for the transition structure is at the B3LYP/6-31G(d) level.

$ClFC=O$  has a higher activation barrier ( $\Delta E^\ddagger = 16.8$  kcal/mol) since the GS complex is more linear with a greater stabilization energy ( $-14.5$  kcal/mol) and the Li-Cl bond is elongated in the TS (Figure 4).

**(b) Methanolysis of Acetyl Chloride.** Nearly two decades ago it was suggested that solvolysis of  $CH_3COCl$  in the presence of an electrophilic catalyst such as phenol may proceed via an ion pair,  $(CH_3CO^+) \cdots (ClHOPh^-)$ , and that solvolysis in methanol involves a loose  $S_N2$  transition state with high carbocation character.<sup>19,20</sup> A more recent experimental paper<sup>2</sup> also suggests that the rate of methanolysis of acetyl chloride exhibits a high sensitivity to changes in solvent ionizing power, a behavior consistent with  $S_N1$ -like C-Cl bond cleavage. Attempts to correlate the rates of solvolysis with known  $S_N1$  substrates such as *tert*-butyl chloride led to a comparison of the experimental enthalpy of chloride ion exchange in

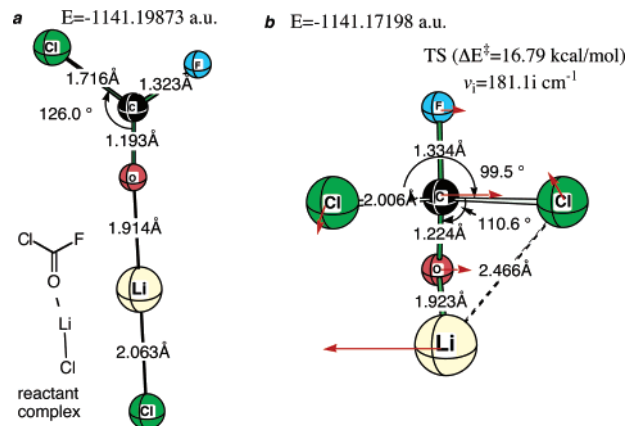
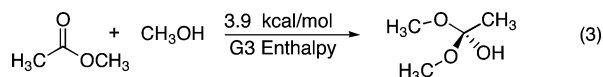
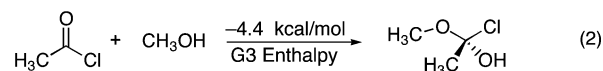
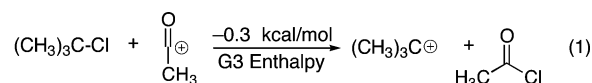


**FIGURE 4.** Exchange reaction of LiCl with  $ClFC=O$ :  $LiCl + ClFC=O \rightarrow LiF + (Cl)_2C=O$ . Reactant complex (a) and transition structure (b) are optimized at the B3LYP/6-31+G(d,p) level. Imaginary frequency for the transition structure is at the B3LYP/6-31G(d) level.

the gas phase that suggests that heterolysis to give acetyl cation is more favorable ( $\Delta H = -3.5 \pm 3$  kcal/mol) than heterolysis of *tert*-butyl chloride, suggesting that an acylium cation is thermodynamically more stable than a *tert*-carbocation. Moreover, in water at 0 °C the solvolysis of acetyl chloride is over  $10^5$  times faster than that of *tert*-butyl chloride.<sup>2</sup>

This led to the suggestion that acetyl cation may benefit more than *tert*-butyl cation from general solvation. An  $S_N2$  mechanism was proposed for both solvolysis and aminolysis of acetyl chloride, and it was suggested that a carbonyl addition pathway was probably not involved and that a strong sensitivity to nucleophilic attack was responsible for this behavior.

Our gas-phase calculations at the G3 level suggest a more thermoneutral chloride ion exchange reaction with acetyl chloride (eq 1), inferring that at least in the gas phase acetyl and *tert*-butyl cations are of comparable stability.



Next we examined the energetics of formation of a tetrahedral intermediate from the condensation of methanol with acetyl chloride (eq 2) and found that the reaction is only slightly exothermic ( $-4.4$  kcal/mol) while addition of methanol to methyl acetate (eq 3) is slightly endothermic. Much to our surprise, when we attempted to form the comparable tetrahedral intermediate from methanol and *protonated* acetyl chloride, it did not collapse to a gas-phase tetrahedral intermediate! Geometry optimization starting with a preformed protonated approximate tetrahedral intermediate with the appropriate bond

(30) (a) Glukhovtsev, M. N.; Pross, A.; Radom, L. *J. Am. Chem. Soc.* **1994**, *116*, 5961. (b) Bach, R. D.; Baboul, A. G.; Schlegel, H. B. *J. Am. Chem. Soc.* **2001**, *123*, 5787 and references therein.

(31) For an earlier study of substitution reactions of the degenerate exchange reactions of  $Cl^-$  with  $HCOCl$  and  $CH_3COCl$  see Blake, J. F.; Jorgensen, W. L. *J. Am. Chem. Soc.* **1987**, *109*, 3856. At the HF/3-21+G level, the tetrahedral adduct and the fully planar  $c_{2v}$  were both found to be transition states. With inclusion of electron correlation [MP3/MP2/6-31+G(d)], the tetrahedral TS was energetically favored. However, the planar  $\sigma$  TS is also a second-order saddle point at the MP2 as well as the B3LYP level. Analytical second derivatives were not available to confirm the earlier saddle points.

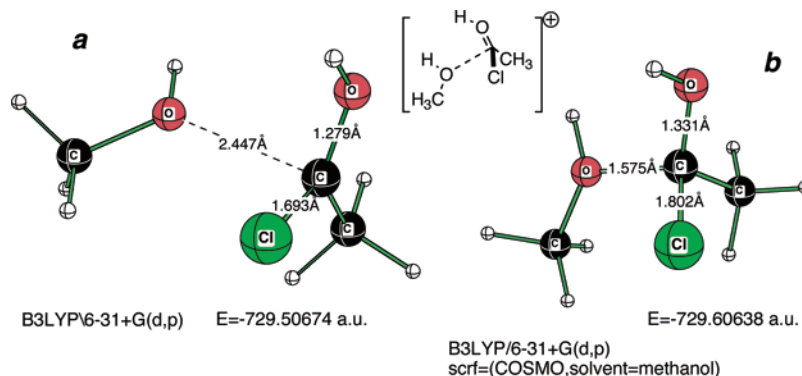


**FIGURE 5.** Complex of one methanol molecule with protonated acetyl chloride,  $\text{CH}_3\text{C}(\text{C}=\text{OH})^+\text{Cl}$ , in gas phase (a) and in methanol medium (b).

angles and distances quickly dissociated into an ion-dipole complex with a methanol oxygen–carbonyl carbon distance of 2.45 Å (Figure 5a). Although this intermediate has a stabilization energy of  $-13.8$  kcal/mol, the carbonyl group is essentially  $\text{sp}^2$  hybridized (the sum of the three angles about the carbonyl carbon is  $358.9^\circ$ ). When this ion-dipole complex is optimized within the COSMO solvent model (solvent =  $\text{CH}_3\text{OH}$ ), the oxygen–carbon distance is reduced to 1.58 Å and the total energy drops 62.5 kcal/mol (Figure 5b) as the intermediate starts to approach a tetrahedral structure ( $\Sigma_{\text{angles}} = 339.6^\circ$ ), where the appropriate sum of the tetrahedral angles should be  $328.5^\circ$ . In both minima the angle of approach of the  $\text{CH}_3\text{OH}$  is approximately perpendicular to the  $\text{COCl}$  plane ( $93.6^\circ$  and  $110.6^\circ$ ). This is a particularly illuminating example since standard textbooks still typically show the hydrolysis or alcoholysis of an acid halide or ester to involve a tetrahedral intermediate. As noted below, this acid-catalyzed pathway requires additional solvent molecules and a long-lived tetrahedral intermediate is not in evidence.

**(c) Role of Specific Solvation on Acetyl Chloride Methanolysis/Hydrolysis.** The fact that a methanol molecule did not form a relatively strong bond to the carbon atom of protonated acetyl chloride does not conform to the generally accepted mechanism for acid chloride alcoholysis. This observation encouraged us to examine the effects of specific solvation upon the loss of chloride ion from protonated acetyl chloride in an  $\text{S}_{\text{N}}1$ -like solvolysis. We located a second minimum for the interaction of methanol with protonated acetyl chloride in addition to that in Figure 5a. In this minimum the proton shifts from the carbonyl oxygen to the methanol oxygen, affording an H-bonded complex (Figure 6a) that is 19.8 kcal/mol lower in energy than the complex in Figure 5a. This proton shift is to be expected since the difference in proton affinities [B3LYP/6-311+G(d,p)+ZPVE,  $\Delta\text{PA} = 4.8$  kcal/mol] for methanol oxygen and the carbonyl oxygen of acetyl chloride is sufficient to induce proton migration.<sup>32</sup> With two H-bonding  $\text{CH}_3\text{OH}$  molecules it was necessary to constrain the  $\text{C}=\text{O}\cdots\text{H}$  proton to be bonded to the carbonyl oxygen in order to get a

“minimum” [Figure 6b, frequency at B3LYP/6-31G(d)]. Full geometry optimization at B3LYP/6-311+G(3df,2p) also resulted in an energy minimum with proton migration from the carbonyl oxygen to the more basic adjacent methanol oxygen. However, when three and four  $\text{CH}_3\text{OH}$  molecules were allowed to freely H-bond to protonated acetyl chloride (Figure 6c,d), we observed a methanol solvated protonated acetyl chloride where the methanol oxygen–carbonyl carbon distances are 1.57 and 1.62 Å. The angle of approach of the  $\text{CH}_3\text{OH}$  to the carbonyl carbon ( $114.4^\circ$  and  $113.6^\circ$ ) is suggestive of a developing tetrahedral intermediate. The carbonyl  $\text{C}=\text{O}$  bond distances in Figure 6a–d increase only slightly from 1.23 to 1.32 Å. Of equal importance, the  $\text{C}-\text{Cl}$  bond distances in these solvated intermediates are elongated at 1.84 Å. The corresponding  $\text{C}-\text{Cl}$  distances in protonated acetyl chloride itself and in the  $\text{CH}_3\text{OH}$  solvated complex (Figure 5a) are 1.69 and 1.80 Å. Thus, the earlier postulations based upon methanol solvolysis data<sup>2</sup> that extensive dissociation of the  $\text{C}-\text{Cl}$  bond occurs in a loose  $\text{S}_{\text{N}}2$ -like TS appears to be consistent with our modeling efforts in the gas phase. These combined experimental and theoretical data strongly suggest that a discrete long-lived tetrahedral intermediate does not appear to be involved even in the case of a highly reactive protonated acid chloride.

The number of methanol molecules was then increased to six in an effort to afford the maximum possibility for the location of a discrete tetrahedral intermediate. Starting with a loosely bound structure resembling that in Figure 6d ( $\text{CH}_3\text{OH}\cdots\text{C}=\text{O} = 1.62$  Å), the six  $\text{CH}_3\text{OH}$  molecules were positioned around the protonated acetyl chloride. As the geometry optimization starts, a proton relay to the adjacent methanol oxygen transpires almost immediately, forming a protonated methanol molecule and an approximate tetrahedral structure [ $\text{CH}_3(\text{OH})\text{C}(\text{OCH}_3)\text{Cl}$ ] is formed (not a minimum). However, the  $\text{C}-\text{Cl}$  bond ionizes, and after many gradient cycles, with considerable movement of the solvent molecules, a stable intermediate with a carbonyl carbon $\cdots\text{Cl}$  distance of 4.627 Å (Figure 7) is eventually located. The adjacent protonated methanol ( $\text{CH}_3-\text{OH}_2^+$ ) is strongly H-bonded to the resulting methyl ester oxygen. The ionized chloride ion is essentially surrounded by solvent molecules. Thus, even with six solvent molecules we see no evidence of a long-lived tetrahedral intermediate. These data nicely corroborate the earlier experimental data that tend to

(32) The proton affinity of methanol at the B3LYP/6-311+G(d,p)+ZPVE level is 178.8 kcal/mol and that of acetyl chloride is 174.0 kcal/mol. The PA of water is lower at 168.9 kcal/mol. The PA of the carbonyl oxygen of methyl acetate is calculated to be 190.9 kcal/mol at this level.

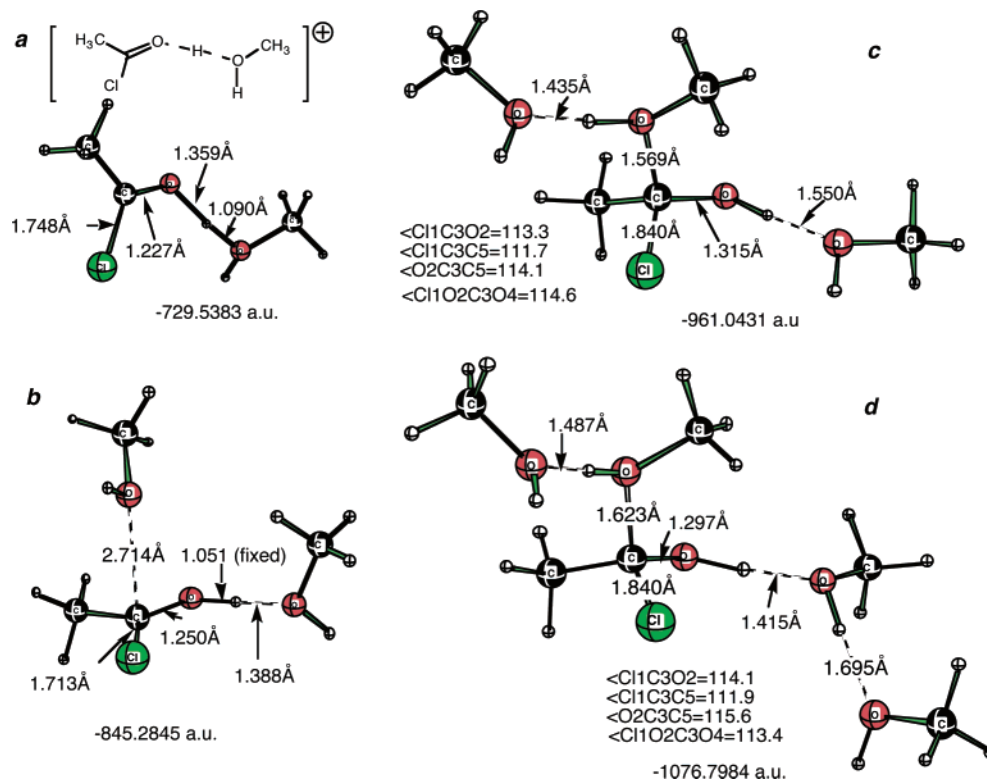


**FIGURE 6.** Complexes of one, two, three, and four methanol molecules with protonated acetyl chloride,  $\text{CH}_3\text{C}(\text{C}=\text{OH})^+\text{Cl}$ , optimized in the gas phase at the B3LYP/6-31+G(d,p) level.

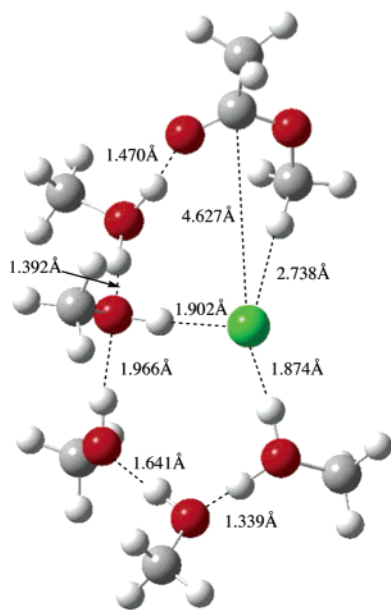


**FIGURE 7.** Final hydrogen-bonded complex of methyl acetate and chloride ion complexed to six methanol molecules, optimized in the gas phase [ $E = -1308.35834$  au, B3LYP/6-31+G(d,p)]. The starting aggregate was protonated acetyl chloride,  $\text{CH}_3\text{C}(\text{C}=\text{OH})^+\text{Cl}$ , loosely complexed to six  $\text{CH}_3\text{OH}$  molecules approximately arranged as presented in Figure 6d.

describe such a scenario leading to the methanolysis product in Figure 7.

We observed comparable results when attempting to model the solvolysis of protonated acetyl chloride in aqueous media. The complexation of protonated acetyl

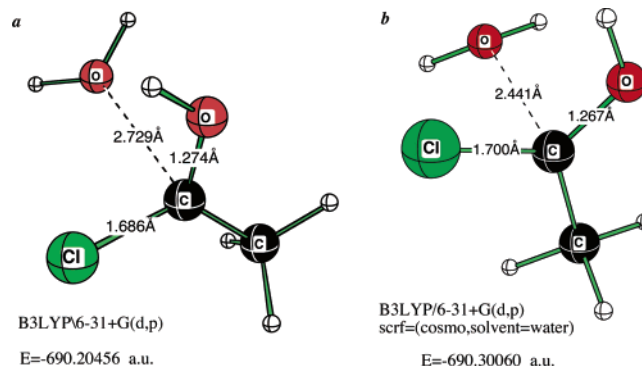


**FIGURE 8.** Complex of protonated acetyl chloride,  $\text{CH}_3\text{C}(\text{C}=\text{OH})^+\text{Cl}$ , with one water molecule in the gas phase (a) and in water solvent (b).

chloride with one water molecule in the gas phase (Figure 8a) and in aqueous solution (COSMO solvent model, Figure 8b) did not collapse to a tetrahedral intermediate. The resulting minima had carbonyl carbon–water oxygen distances well in excess of 2 Å. We also observe partial ionization of the carbonyl carbon–chloride distance when this protonated functional group is surrounded by six water molecules (Figure 9a). When a proton relay occurred, the resulting hydronium ion was strongly H-bonded to several neighboring water molecules. In this case the water molecule is slightly less basic than acetyl chloride.<sup>32</sup> As a result of such secondary bonding interactions, the potential energy surface (PES) is very soft and these structures obviously do not represent global minima, but they were fully optimized without geometry constraints. These combined data suggest that a series of



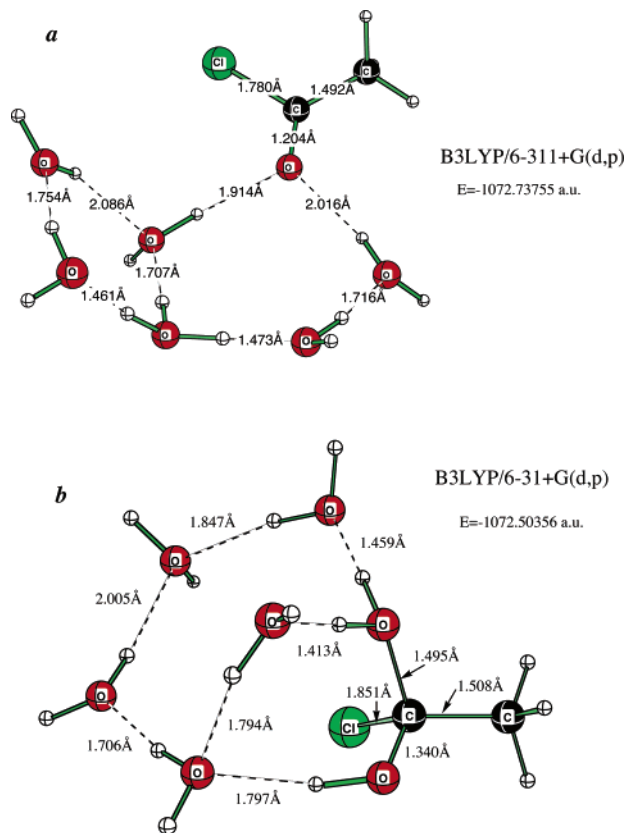


**FIGURE 9.** Complex of protonated acetyl chloride,  $\text{CH}_3\text{C}(\text{C}=\text{OH})^+\text{Cl}$ , with six water molecules with (a) and without a proton relay (b) optimized in gas phase. Structure a is 16.3 kcal/mol lower in energy than structure b; at the B3LYP/6-31+G(d,p) level  $E[\text{a}] = -1072.529\ 60$  au.

proton relays effect the alcoholysis of this highly reactive acid chloride and that a long-lived tetrahedral intermediate is not essential to the overall reaction pathway.

**(d) Acid-Catalyzed Acyl Transfer Reactions with Methyl Acetate.** The C–X bond strength of the leaving group obviously plays a major role in determining the mechanism of acyl transfer. Since an alkoxide has been deemed a very poor nucleofuge in all types of S<sub>N</sub>2 reactions, we carried out a comparative study on acyl transfer with methyl acetate. Acid catalysis with esters requires a very strong acid due to the weakly basic nature of the carbonyl group. The proton affinity (PA) of the carbonyl oxygen of methyl acetate is calculated to be 192.8 kcal/mol at the B3LYP/6-311+G(3df,2p) level. By comparison, the protonation of methanol gives a PA for CH<sub>3</sub>OH of 178.4 kcal/mol at this level. Interestingly, the PA of the alcohol oxygen of methyl acetate is much lower than that of the carbonyl oxygen at 177.3 kcal/mol. CH<sub>3</sub>O protonated methyl acetate is partially dissociated into methanol and the acylium ion ( $^+\text{O}=\text{C}\cdots\text{OCH}_3 = 1.73$  Å), providing additional evidence that this acetyl cation is more stable than we had imagined previously (eq 1). As noted above (eq 3), the formation of a tetrahedral intermediate from the condensation of methyl acetate and methanol is slightly endothermic. We also find that methanol does not form a tetrahedral intermediate with protonated methyl acetate in much the same manner noted above for protonated acetyl chloride (Figure 5). Attempted geometry optimization of such an intermedi-

ate gave a methanol oxygen–carbonyl carbon distance of 2.743 Å; this gas-phase ion–dipole complex has a stabilization energy of  $-15.7$  kcal/mol [B3LYP/6-31+G(d,p)] (Figure 10). Geometry optimization within the COSMO solvent model<sup>37b</sup> (solvent = methanol) still did not effect collapse to a tetrahedral intermediate and the O=C⋯O distance remained at 2.58 Å. A similar situation was observed with attempts to get a water molecule to collapse to a well-defined tetrahedral intermediate (Figure 10C,D). The water molecule is moderately bound to the carbonyl carbon with a binding energy of  $-15.6$  kcal/mol. Again we observe that the presence of six solvent molecules (CH<sub>3</sub>OH) does not result in the formation of a tetrahedral intermediate and the closest distance of the methanol oxygen to the carbonyl carbon of protonated methyl acetate is 3.867 Å (Figure 11). Despite the differences in proton affinities of the carbonyl oxygen and methanol, a proton relay is noted but with a very strong H-bond to the adjacent carbonyl oxygen ( $r = 1.321$  Å), which sets up a second strong H-bond to its closest methanol oxygen (1.510 Å). The lack of methoxide exchange in this solvated minimum clearly reflects the strength of the C–OCH<sub>3</sub> bond even under acidic conditions. On the basis of these observations, one may also question the formation of a long-lived tetrahedral intermediate at the active site of an enzyme.

**(e) Base-Catalyzed Acyl Transfer Reactions with Methyl Acetate.** In addition to the acid-catalyzed methods for acyl transfer, a great many reactions are commonly carried out under basic conditions. In an exemplary theoretical study, Ornstein and co-workers<sup>33</sup> suggested that the base-catalyzed saponification of methyl acetate (CH<sub>3</sub>COOCH<sub>3</sub>) proceeds via a tetrahedral intermediate in the gas phase. Their potential energy surface at the QCISD(T)/6-311++G(d,p)//MP2/6-31++G(d,p) level suggests that as hydroxide ion approaches the carbonyl carbon of methyl acetate, it first forms a stable complex with HO<sup>−</sup> hydrogen-bonding to the methyl groups of CH<sub>3</sub>COOCH<sub>3</sub> ( $\Delta E_{\text{stab}} = -17.7$  kcal/mol) before progressing to the TS for addition with a very low activation barrier ( $\Delta E^\ddagger = 0.6$  kcal/mol) for formation of a tetrahedral intermediate. A second TS involving expulsion of methoxide ion (CH<sub>3</sub>O<sup>−</sup>) following an intramolecular proton transfer from the OH to the carbonyl oxygen had a much larger activation barrier of 8.0 kcal/mol. On the contrary, earlier experimental studies suggest that the alkaline hydrolysis of substituted methyl benzoates proceeds in the absence of carbonyl oxygen exchange.<sup>7</sup> It has been proposed<sup>18</sup> that exchange reactions of alkyl esters could change from one with a TS resembling a tetrahedral intermediate to one involving a discrete tetrahedral intermediate when the leaving group reaches a pK<sub>a</sub> of 10. We elected to take a closer look with methoxide ion as the nucleophile to take advantage of the symmetry of the potential intermediates on the PES for CH<sub>3</sub>O<sup>−</sup> addition to methyl acetate.

We located a reactant minimum ( $\Delta E_{\text{stab}} = -11.9$  kcal/mol) where the methoxide ion was H-bonded to the methyl groups of methyl acetate (B3LYP/6-311+G(3df,2p)). The TS for the addition of methoxide ion to the carbonyl carbon (TS1 in Figure 12) had a very small

(33) Zhan, C.-G.; Landry, D. W.; Ornstein, R. L. *J. Am. Chem. Soc.* **2000**, *122*, 1522.

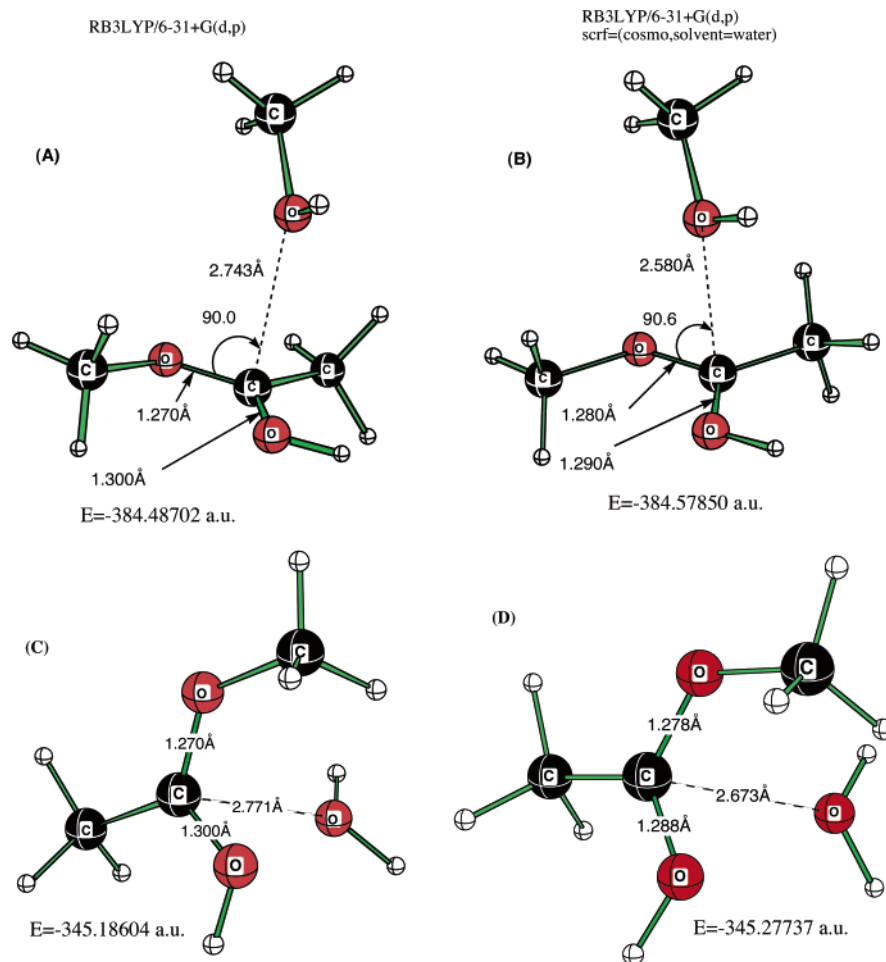


**FIGURE 10.** Complex of one methanol molecule with protonated  $[\text{CH}_3(\text{C}=\text{OH})\text{OCH}_3]^+$  in the gas phase (A) and in methanol medium (B) optimized at the B3LYP/6-31+G(d,p) level of theory. Minima C and D represent complexation of a single water molecule with protonated methyl acetate [geometry optimization is at the B3LYP/6-31+G(d,p) level]. Structures B and D were optimized by the COSMO method.<sup>37b</sup>

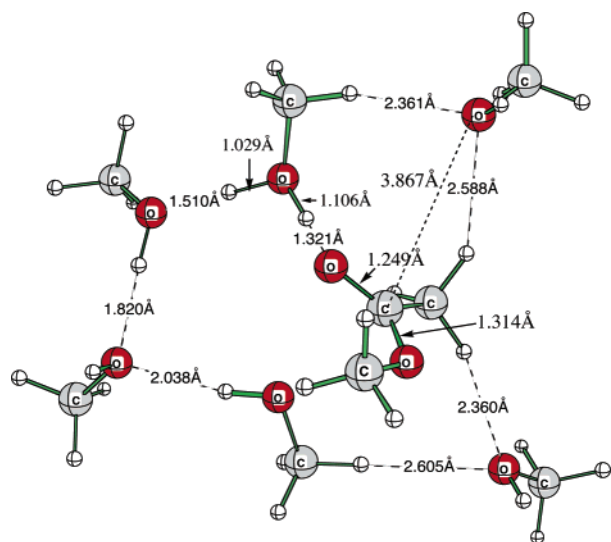


**FIGURE 11.** Complex of six methanol molecules with protonated  $[\text{CH}_3(\text{C}=\text{OH})\text{OCH}_3]^+$  in the gas-phase optimized at the B3LYP/6-31+G(d,p) level of theory ( $E = -963.26428$  au).

activation barrier ( $\Delta E^\ddagger = 0.6$  kcal/mol). However, the product of nucleophilic addition is not the anticipated

*symmetrical* tetrahedral intermediate but rather an asymmetrical adduct (AI in Figure 12) with differing carbonyl carbon–methoxide oxygen ( $\text{O}=\text{C}-\text{OCH}_3$ ) distances of 1.483 and 1.564 Å. This structure exhibits significant ion–dipole character with the carbonyl group intact ( $\text{C}=\text{O}$  distance is 1.264 Å in this adduct versus 1.204 Å in  $\text{CH}_3\text{COOCH}_3$ ). We were also able to locate an essentially symmetrical tetrahedral intermediate (SI in Figure 12) for addition of  $\text{CH}_3\text{O}^-$  to  $\text{CH}_3\text{COOCH}_3$  without geometry constraints ( $\text{O}=\text{C}-\text{OCH}_3$  distances of 1.523 and 1.538 Å). However, this symmetric intermediate is 2.60 kcal/mol *higher in energy* than the above asymmetrical tetrahedral intermediate and is only slightly lower in energy than the reactant complex (RC in Figure 12).

We have yet to locate a transition state that separates the two identical asymmetrical intermediates (AI) on the reaction coordinate in Figure 12. It is most intuitive that the observed symmetrical intermediate (SI) would lie on the reaction pathway and would therefore be separated from the asymmetrical intermediates by two identical, asymmetrical transition states. However, we have no evidence that the symmetrical intermediate lies on the reaction pathway, and therefore it cannot be ruled out that the asymmetrical intermediates are actually separated by a symmetrical transition state (the dashed red



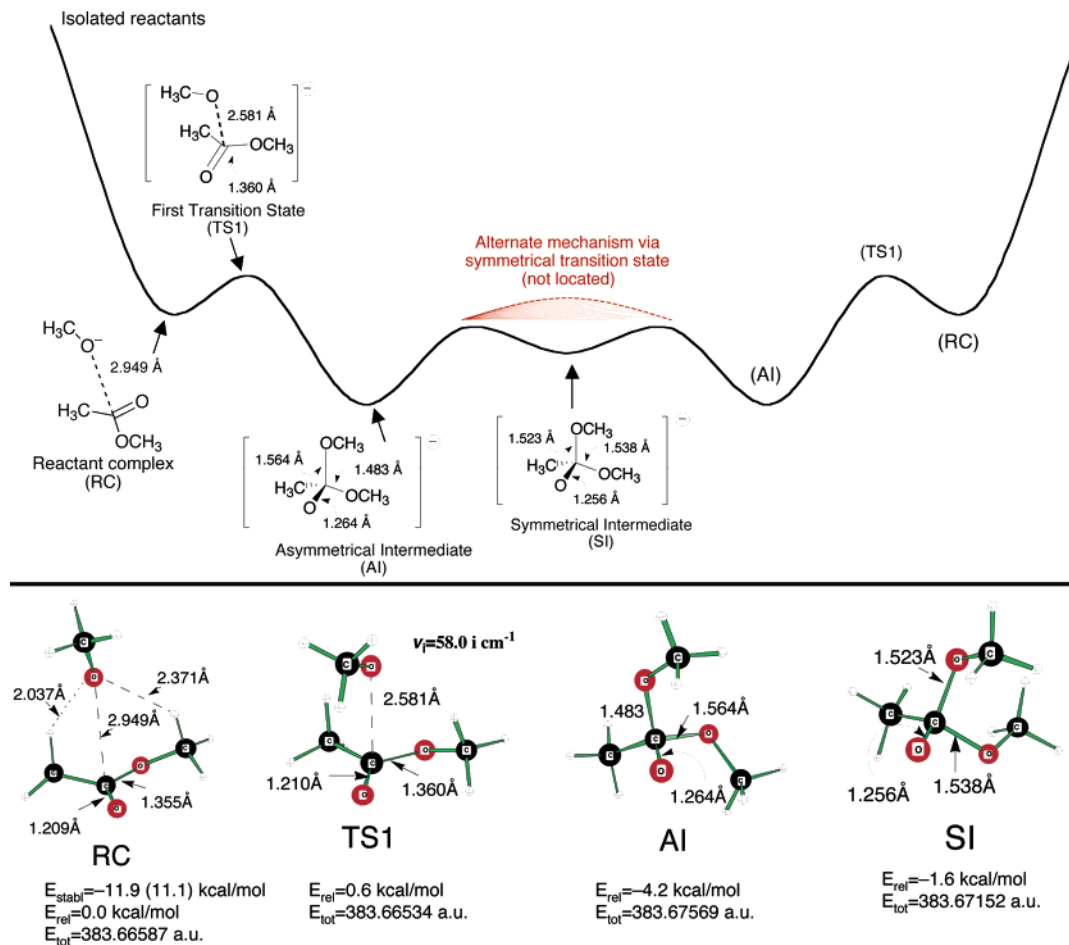
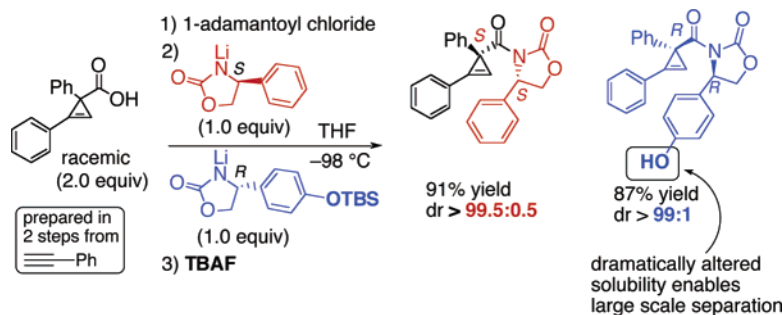


**FIGURE 12.** Multiple-well energy surface for the reaction of methyl acetate with methoxide ion. Shown are minimized structures and energies of the reactant complex (RC), the transition structure for  $\text{CH}_3\text{O}^-$  addition to the carbonyl carbon of  $\text{CH}_3\text{COOCH}_3$  (TS1), and an unsymmetrical intermediate (AI) and an essentially symmetrical tetrahedral intermediate (SI) optimized at the B3LYP/6-311+G(3df,2p) level of theory. Reaction energetics are given in kilocalories per mole and are relative to the total energy of the isolated reactants. The numbers in parentheses are at the B3LYP/6-311+G(3df,2p)+ZPVE level.

## SCHEME 2. Parallel Kinetic Resolution of Cyclopropene Carboxylic Acids



line in Figure 12). In either case, the observation is a multiple-well energy surface<sup>13</sup> rather than a single intermediate.

**(f) Model Synthetic Studies Involving Acyl Transfer.** Now that we have a better understanding of when to expect a concerted acyl transfer reaction, we can apply these principles to some more complex synthetic applications. Enantio- and diastereoselective methods for acyl transfer are important reactions for kinetic resolution and asymmetric desymmetrization.<sup>26–29</sup> As a part of a synthetic program to develop useful new reaction chem-

istry of strained molecules, we recently developed a parallel kinetic resolution strategy for resolving multi-gram quantities of cyclopropene carboxylic acids (Scheme 2).<sup>34</sup> Importantly, Scheme 2 represents a new type of parallel kinetic resolution in which quasienantiomers with very similar reactivities give products whose chromatographic properties diverge after treatment with fluoride. To improve the scope of this parallel kinetic

(34) Liao, L.-a.; Zhang, F.; Dmitrenko, O.; Bach, R. D.; Fox, J. M. *J. Am. Chem. Soc.* **2004**, *126*, 4490.

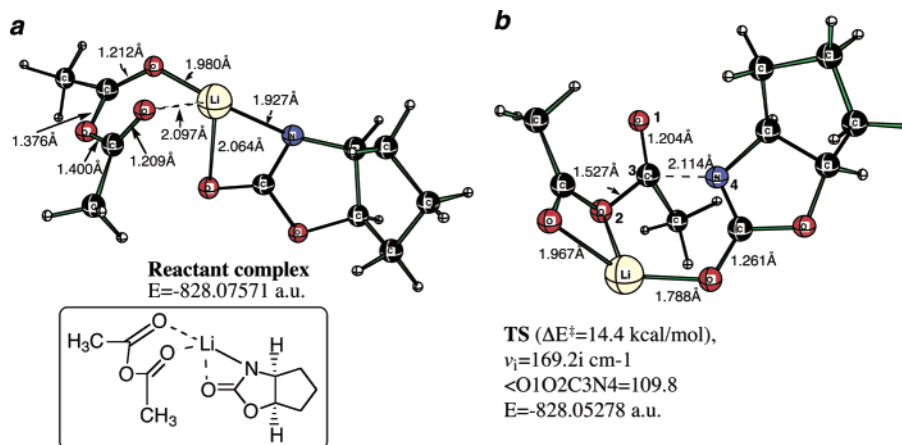


**FIGURE 13.** Reactant complex and TS for the reaction of acetic anhydride (as the acyl-transfer agent) and the N-lithiated oxazolidinone from *cis*-1-amino-2-cyclopentanol as the nucleophile.

resolution, we hoped to develop computational models that could explain the diastereoselectivity of the acyl transfer process. We recently accomplished this with the B3LYP functional employing the 6-31+G(d,p) basis set and reported the model in accompaniment with full details of the experimental work.<sup>34</sup> The computational design was nontrivial: each diastereomer contains more than 35 heavy atoms, and a systematic study of a smaller model system was required before eventual calculations on the “real” system. Below, we describe the full details of the computational aspects of the parallel kinetic resolution.

**II.2. Model Study for Parallel Kinetic Resolution: Reaction of a Chiral Oxazolidinone with Acetic Anhydride.** To develop a mechanistic basis for optimizing the process in Scheme 2, it was first necessary to understand the mechanism of the acyl transfer step. Since a carboxylate is a moderate leaving group, the above discussion would tend to discourage the suggestion of the more typically assumed addition–elimination process in favor of a concerted displacement at carbonyl carbon. Furthermore, a computational study of *N*-acyloxazolidinone formation from anhydrides would have broad significance because oxazolidinone auxiliaries are widely used to induce asymmetry in the reactions of enolates.<sup>35</sup> We report here theoretical evidence that anhydrides react with Li oxazolidinones via an approximately tetrahedral *transition state*.

In our initial model theoretical studies we have used acetic anhydride as the acyl transfer agent and the N-lithiated oxazolidinone from *cis*-1-amino-2-cyclopentanol as the nucleophile. The pre-reaction complex that we found is not necessarily the global minimum, but rather we chose a structure that was close to the TS in its orientation of the nucleophilic nitrogen with respect to the carbonyl carbon (Figure 13). Structures are optimized at the RB3LYP/6-31+G(d,p) level of theory. Imaginary frequency for the transition structure is at the B3LYP/6-31G(d) level.

The lithium cation is bonded closely to the basic nitrogen site as well as to the amide oxygen atom. Both

carbonyl oxygens of the acetic anhydride are also complexed to the lithium atom. The overall stabilization energy relative to isolated reactants is rather large (−128.6 kcal/mol) since the coulombic interaction of oppositely charged particles is also involved. The TS for acyl transfer is clearly a  $\pi$  attack of the nucleophilic oxazolidinone nitrogen approaching in a nearly perpendicular manner to the electrophilic acyl group at an angle of 109.8° in much the same manner as the attack of Cl<sup>−</sup> on acetyl chloride (Figure 1). The classical activation barrier of 14.4 kcal/mol suggests a rather facile acyl transfer reaction. A frequency calculation on the TS (Figure 13) clearly confirms the reaction to be a concerted first-order process with *both* C–N bond making and C–O bond breaking comprising the reaction vector that has a single imaginary frequency (169.2i cm<sup>−1</sup>). No evidence of a tetrahedral intermediate could be found despite several such attempts.

Since the reaction conditions often include the addition of LiCl as a catalyst,<sup>36</sup> we also located the TS for acyl transfer in the presence of LiCl (Figure 14). The pre-reaction complex ( $\Delta E_{\text{stab}} = 175.2$  kcal/mol) that we were able to locate (Figure 14), however, does not resemble the TS; it is more extended. The chloride is bound to both lithium ions, and nucleophilic nitrogen is complexed to lithium. These relatively strong ionic interactions serve to lower the ground-state energy and correspondingly increase the activation barrier. Additionally, the acyl group is more remote from the nucleophilic nitrogen and the TS for acyl transfer has a rather coiled structure. The loss of several of these stabilizing interactions in the TS for acyl transfer also contributes to an increase in the activation barrier ( $\Delta E^\ddagger = 34.4$  kcal/mol). In the TS, the LiCl molecule is involved only in bonding to the carbonyl oxygen of the transferring acyl group. Nonetheless, this is still a concerted acyl transfer reaction with an approach of the nucleophilic nitrogen to the developing carboxylate plane of 106.9°. The reaction vector (163.7i cm<sup>−1</sup>) has a larger component of C–N bond formation and a lesser contribution of C–O bond cleavage due to electrophilic activation by LiCl, but both are still present.

(35) Ager, D. J.; Prakash, I.; Schaad, D. R. *Chem. Rev.* **1996**, *96*, 835.

(36) Ho, G.-J.; Mathre, D. J. *J. Org. Chem.* **1995**, *60*, 2271.

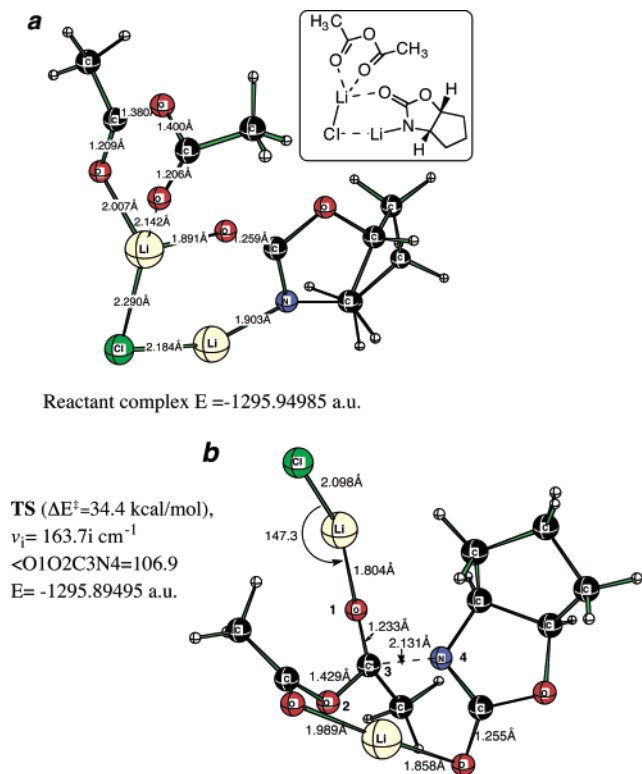


**FIGURE 14.** Reactant complex and TS for the reaction of acetic anhydride (as the acyl-transfer agent) and the N-lithiated oxazolidinone from *cis*-1-amino-2-cyclopentanol in the presence of LiCl. Structures are optimized at the RB3LYP/6-31+G(d,p) level of theory. Imaginary frequency for the transition structure is at the B3LYP/6-31G(d) level.

The developing C–N distance is 2.13 Å and the distance of the C–O bond of the departing carboxylate is 1.43 Å.

**II.3. Parallel Kinetic Resolution of a Cyclopropane Carboxylic Acid: Analysis of Diastereomeric Transition States and Correlation to Experimental Observation.** Having established a concerted mechanism for the acyl transfer reactions of lithiated oxazolidiones with acetic anhydride, we next studied the diastereoselective reaction described in Scheme 2. For these calculations, we studied the real system of *S*-4-phenyloxazolidinone in separate experiments with both enantiomers of 1,3-diphenylcycloprop-1-ene carboxylic acid. Calculations were performed with the B3LYP functional with the 6-31+G(d,p) basis set. The development of the models in Figure 15 was multilayered. Structures were built from the coordinates from Figure 14, and multiple trajectories of nucleophilic attack were considered. The only modification from the experimental system is that *t*-Bu was used in place of adamantyl in the calculations. The lowest energy *transition states* for each diastereomer are displayed in Figure 15. In accord with the experimental observation, the transition state that leads to the major product is calculated to be lower in energy by 1.1 kcal. Both transition structures are characterized by single imaginary frequencies around 172i cm<sup>-1</sup>, the animation of which indicates *both* concerted C–N bond formation and C–O bond cleavage. The diastereomeric transition states are shown in Figure 15.

The transition states in Figure 15 are remarkably similar despite their diastereomeric relationship. This

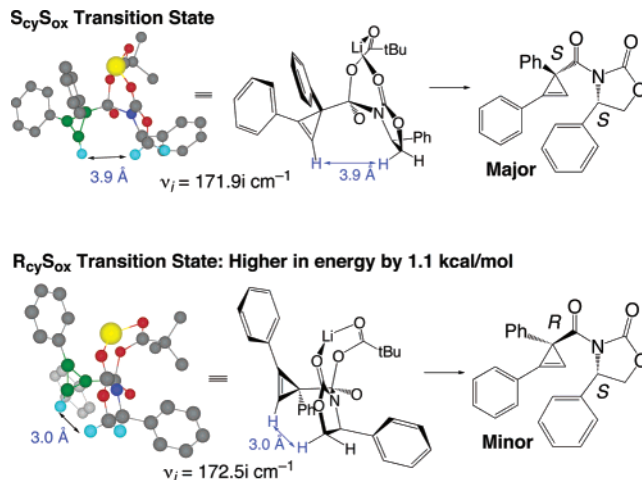


**FIGURE 15.** Diastereomeric transition states for acyl transfer from the *tert*-butyl anhydride of 1,3-diphenylcycloprop-1-ene carboxylic acid to the lithium salt of 4-phenyloxazolidinone. Structures are optimized at the RB3LYP/6-31+G(d,p) level of theory. Imaginary frequency for the transition structure is at the same level.

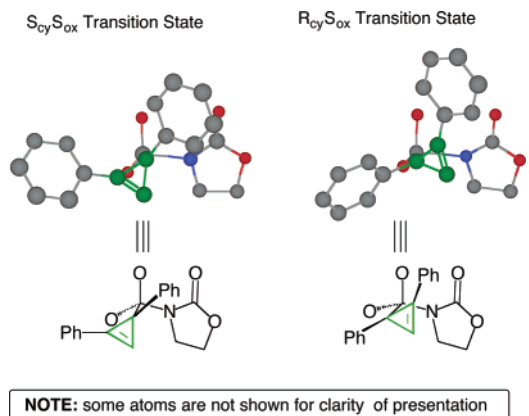


**FIGURE 16.** Alternative view of the core structures of the diastereomeric transition structures from Figure 15. Many of the atoms were deleted to demonstrate the similarities between the transition states.

point becomes readily apparent when the core structures (without the lithium atoms, pivaloyl groups, or oxazolidione substituents) are compared as shown in Figure 16. The two transition states are related by an approximate 60° rotation about the bond that joins the acyl carbon to the cyclopropane. The structural similarities and complex nature of the two transition states makes it unlikely that less sophisticated models could predict the diastereoselectivity. However, B3LYP/6-31+G(d,p) calculations predict the energy of the *R<sub>cy</sub>S<sub>ox</sub>* isomer to be 1.1 kcal higher in energy than the *S<sub>cy</sub>S<sub>ox</sub>* diastereomer—in close accord with the experimental observation.<sup>34</sup> Despite the similarities, there are notable differences between the two structures that should be useful for further optimizing the selectivity. For example, the distance between the alkene hydrogen and that of C5 of the oxazolidinone in *S<sub>cy</sub>S<sub>ox</sub>* is 3.9 Å, whereas it is only 3.0 Å for *R<sub>cy</sub>S<sub>ox</sub>* (Figure 15). In future work, we will be able to exploit this observation to develop even more selective and general systems for parallel kinetic resolu-



tion and thereby increase the utility of chiral cyclopropanes in the synthesis of natural products and druglike molecules.

### III. Conclusions

Chloride ion exchange reactions with both formyl and acetyl chloride proceed by a  $\pi$  attack on the C=O bond with no discernible tetrahedral intermediate typical of an addition–elimination pathway. While a tetrahedral intermediate does exist for the addition of fluoride ion to (Cl)<sub>2</sub>C=O, halide exchange of LiCl with both ClFC=O and (Cl)<sub>2</sub>C=O proceeds by a concerted S<sub>N</sub>2-like pathway. The formation of a tetrahedral intermediate from the addition of methanol to acetyl chloride is slightly exothermic (–4.4 kcal/mol), while the addition of methanol to the carbonyl group of methyl acetate is slightly endothermic (3.9 kcal/mol). Even when six CH<sub>3</sub>OH molecules are H-bonded to protonated acetyl chloride, a tetrahedral intermediate is not in evidence and this solvated complex is consistent with an S<sub>N</sub>1-type ionization of Cl<sup>–</sup>. These results corroborate earlier suggestions that the methanolysis of acetyl chloride does not proceed through the generally assumed addition–elimination pathway. The reluctance to form a tetrahedral intermediate derives from the large difference between the energies of a carbonyl  $\pi$  bond and a C–O single bond. In the absence of extensive solvation at carbonyl oxygen, the C=O resists conversion to a C–O single bond. Thus the C–X bond strength and the stability of the leaving group have a profound effect upon the mechanism of acyl transfer reactions as evidenced by the difference in the overall reaction coordinate for acid chlorides versus

methyl esters. These observations are reminiscent of the S<sub>N</sub>1–S<sub>N</sub>2 variable alkyl halide solvolysis transition-state arguments of the late 1960s.<sup>1</sup>

The reaction of methoxide ion with methyl acetate proceeds via a multiple-well energy surface and involves the intermediacy of an asymmetrical species with differing C–OCH<sub>3</sub> bond lengths. Models of synthetic applications of acyl transfer involving anhydrides also proceed by a concerted S<sub>N</sub>2-type pathway that involves a good nucleophile and a moderate carboxylate leaving group. The TS for acyl transfer from acetic anhydride to the nucleophilic nitrogen of N-lithiated oxazolidinone, derived from *cis*-1-amino-2-cyclopentanol, involves a nearly perpendicular attack on the  $\pi$  bond of the electrophilic acyl group in much the same manner as the attack of Cl<sup>–</sup> on acetyl chloride. A frequency calculation on the TS clearly confirms the reaction to be a concerted first-order process involving *both* C–N bond making and C–O bond breaking in the transition state. Concerted transition states were also observed for the reactions of each enantiomer of a 1,3-diphenylcycloprop-2-ene carboxylic anhydride by *S*-3-lithio-4-phenyloxazolidinone. Despite close structural similarities between the diastereomeric transition states, the relative energies correlated closely with the experimental results.

### IV. Computational Details

Quantum chemistry calculations were carried out by use of the Gaussian98 program system<sup>37a</sup> with gradient geometry optimization.<sup>38</sup> All geometries were fully optimized by use of the B3LYP functional<sup>39,40</sup> with 6-31G(d), 6-31+G(d,p), and 6-311+G(d,p) basis sets and in some cases by use of COSMO solvation model (polarizable conductor model).<sup>37b</sup> Vibrational frequency calculations were performed to characterize the stationary points as either minima or transition structures (first-order saddle point). Proton affinities (PA) were estimated at the B3LYP/6-31+G(d,p), B3LYP/6-311+G(d,p), and B3LYP/6-311+G(3df,2p) levels of theory with the inclusion of the zero-point vibrational energies (ZPVE). The reaction enthalpies were calculated by G3 calculations.<sup>41</sup>

**Acknowledgment.** This work was supported by the National Science Foundation (CHE-0138632) and by National Computational Science Alliance under CHE-990021N and utilized the NCSA SGI Origin2000 and University of Kentucky HP Superdome. The experimental work was supported by NIH Grant P20 RR017716-01 from the COBRE Program of the National Center for Research Resources.

**Supporting Information Available:** Cartesian coordinates and total energies are available for the minima and transition states described in this work. This material is available free of charge via the Internet at <http://pubs.acs.org>.

JO049494Z

(37) (a) Frisch, M. J.; Trucks, G. W.; Schlegel, H. B.; Scuseria, G. E.; Robb, M. A.; Cheeseman, J. R.; Zakrzewski, V. G.; Montgomery, J. A.; Stratmann, R. E.; Burant, J. C.; Dapprich, S.; Millam, J. M.; Daniels, A. D.; Kudin, K. N.; Strain, M. C.; Farkas, O.; Tomasi, J.; Barone, V.; Cossi, M.; Cammi, R.; Mennucci, B.; Pomelli, C.; Adamo, C.; Clifford, S.; Ochterski, J.; Petersson, G. A.; Ayala, P. Y.; Cui, Q.; Morokuma, K.; Malick, D. K.; Rabuck, A. D.; Raghavachari, K.; Foresman, J. B.; Cioslowski, J.; Ortiz, J. V.; Baboul, A. G.; Stefanov, B. B.; Liu, G.; Liashenko, A.; Piskorz, P.; Komaromi, I.; Gomperts, R.; Martin, R. L.; Fox, D. J.; Keith, T.; Al-Laham, M. A.; Peng, C. Y.; Nanayakkara, A.; Gonzalez, C.; Challacombe, M.; Gill, P. M. W.; Johnson, B.; Chen, W.; Wong, M. W.; Andres, J. L.; Gonzalez, C.; Head-Gordon, M.; Replogle, E. S.; Pople, J. A. *Gaussian 98*, Revision A.7; Gaussian, Inc.: Pittsburgh, PA, 1998. (b) Barone, V.; Cossi, M.; Tomasi, J. *J. Comput. Chem.* **1998**, *19*, 404.

(38) (a) Schlegel, H. B. *J. Comput. Chem.* **1982**, *3*, 214. (b) Schlegel, H. B. *Adv. Chem. Phys.* **1987**, *67* (Pt. 1), 249. (c) Schlegel, H. B. In *Modern Electronic Structure Theory*; Yarkony, D. R., Ed.; World Scientific: Singapore, 1995; p 459.

(39) (a) Becke, A. D. *Phys. Rev. A* **1988**, *38*, 3098. (b) Lee, C.; Yang, W.; Parr, R. G. *Phys. Rev. B* **1988**, *37*, 785.

(40) (a) Becke, A. D. *J. Chem. Phys.* **1993**, *98*, 5648. (b) Stevens, P. J.; Devlin, F. J.; Chabalowski, C. F.; Frisch, M. J. *J. Phys. Chem.* **1994**, *98*, 11623.

(41) Curtiss, L. A.; Raghavachari, K.; Redfern, P. C.; Rassolov, V.; Pople, J. A. *J. Chem. Phys.* **1998**, *109*, 7764.